



Cancer Research

Targets of the Tumor Suppressor *miR-200* in Regulation of the Epithelial –Mesenchymal Transition in Cancer

Mark J. Schliekelman, Don L. Gibbons, Vitor M. Faca, et al.

Cancer Res 2011;71:7670-7682. Published OnlineFirst October 10, 2011.

Updated version Access the most recent version of this article at:
doi:[10.1158/0008-5472.CAN-11-0964](https://doi.org/10.1158/0008-5472.CAN-11-0964)

Supplementary Material Access the most recent supplemental material at:
<http://cancerres.aacrjournals.org/content/suppl/2011/12/13/0008-5472.CAN-11-0964.DC1.html>

Cited Articles This article cites by 46 articles, 13 of which you can access for free at:
<http://cancerres.aacrjournals.org/content/71/24/7670.full.html#ref-list-1>

Citing articles This article has been cited by 4 HighWire-hosted articles. Access the articles at:
<http://cancerres.aacrjournals.org/content/71/24/7670.full.html#related-urls>

E-mail alerts [Sign up to receive free email-alerts](#) related to this article or journal.

Reprints and Subscriptions To order reprints of this article or to subscribe to the journal, contact the AACR Publications Department at pubs@aacr.org.

Permissions To request permission to re-use all or part of this article, contact the AACR Publications Department at permissions@aacr.org.

Targets of the Tumor Suppressor *miR-200* in Regulation of the Epithelial–Mesenchymal Transition in Cancer

Mark J. Schliekelman¹, Don L. Gibbons^{2,3}, Vitor M. Faca¹, Chad J. Creighton⁴, Zain H. Rizvi², Qing Zhang¹, Chee-Hong Wong¹, Hong Wang¹, Christin Ungewiss², Young-Ho Ahn², Dong-Hoon Shin², Jonathan M. Kurie², and Samir M. Hanash¹

Abstract

The microRNA-200 (miR-200) family restricts epithelial–mesenchymal transition (EMT) and metastasis in tumor cell lines derived from mice that develop metastatic lung adenocarcinoma. To determine the mechanisms responsible for EMT and metastasis regulated by this microRNA, we conducted a global liquid chromatography/tandem mass spectrometry analysis to compare metastatic and nonmetastatic murine lung adenocarcinoma cells which had undergone EMT because of loss of miR-200. An analysis of syngeneic tumors generated by these cells identified multiple novel proteins linked to metastasis. In particular, the analysis of conditioned media, cell surface proteins, and whole-cell lysates from metastatic and nonmetastatic cells revealed large-scale modifications in the tumor microenvironment. Specific increases were documented in extracellular matrix (ECM) proteins, peptidases, and changes in distribution of cell adhesion proteins in the metastatic cell lines. Integrating proteomic data from three subproteomes, we defined constituents of a multilayer protein network that both regulated and mediated the effects of TGF β . Lastly, we identified ECM proteins and peptidases that were directly regulated by miR-200. Taken together, our results reveal how expression of miR-200 alters the tumor microenvironment to inhibit the processes of EMT and metastasis. *Cancer Res*; 71(24); 7670–82. ©2011 AACR.

Introduction

The process of epithelial–mesenchymal transition (EMT) characterized by loss of intercellular adhesion and polarity, cytoskeletal reorganization that enhances cell motility, and degradation of the basement membrane has been associated with tumor progression and metastasis (1). Diverse signaling pathways regulate EMT; TGF β and RAS are capable of inducing EMT in most epithelial cell lines, whereas other pathways such as Wnt/ β -catenin, Notch, and NFK- β have also been shown to regulate EMT (2). Induction of EMT functions in particular through downregulation of the epithelial adhesion protein E-cadherin (CDH1) and direct repression of *Cdh1* has been shown to be under the control of transcriptional regulators ZEB1, ZEB2, TWIST1, SNAIL, and SLUG, which also regulate a large number of other epithelial-related genes (3).

The importance of noncoding microRNAs (miRNA) in tumor development and progression has become increasingly evident. Several miRNAs have been identified as either oncogenes (miR-17-92, miR-155, and miR-21) or tumor suppressors (miR-15a, miR-16a, and let-7), and some human tumor types can be classified by miRNA signatures (4). The miR-200 family of miRNAs consists of 5 members (miR-200b, miR-200a, miR-429, and miR-200c, 141) that have been shown to have a role in EMT in both normal and malignant cells through double-negative feedback regulation with the ZEB transcription factors and regulation of *Cdh1* and vimentin expression (5). This miRNA family has also been shown to have pleiotropic effects, including regulation of stem cell factors and features, indicative of their importance for tissue homeostasis.

We recently showed the importance of miR-200 in EMT and metastasis in a study of metastatic and nonmetastatic tumors from a (*Kras*, *p53*) murine lung adenocarcinoma model (6). This genetic model has biological features and a global metastatic expression profile that is predictive of poor outcome in early-stage lung cancer (7, 8). Cell lines with high or low metastatic potential were established from these mutant *Kras* and *p53* lung adenocarcinoma tumors, and metastatic tumors displayed a high degree of plasticity, exhibiting characteristics of EMT in tumors and 2-dimensional culture (notably in response to EMT-inducing factors such as TGF β), but reexpressing epithelial markers and organizing into normal epithelial structures in laminin-rich 3D Matrigel culture. miRNA profiling of tumors with high metastatic potential revealed loss of miR-200 as a likely regulator of metastatic potential and overexpression of the

Authors' Affiliations: ¹Fred Hutchinson Cancer Research Center, Seattle, Washington; Departments of ²Thoracic/Head and Neck Medical Oncology and ³Molecular and Cellular Oncology, The University of Texas MD Anderson Cancer Center; and ⁴Dan L. Duncan Cancer Center, Baylor College of Medicine, Houston, Texas

Note: Supplementary data for this article are available at Cancer Research Online (<http://cancerres.aacrjournals.org/>).

Corresponding Author: Samir M. Hanash, Fred Hutchinson Cancer Research Center, 1100 Fairview Avenue N., Seattle, WA 98109. Fax: 206-667-2537; E-mail: shanash@fhcrc.org

doi: 10.1158/0008-5472.CAN-11-0964

©2011 American Association for Cancer Research.

miR-200b locus in highly metastatic cells eliminated their ability to undergo EMT and metastasize.

In this work, we have carried out an in-depth comparative proteomic analysis of cells and tumor tissue derived from lung adenocarcinoma tumors that have undergone EMT and have a high metastatic potential to identify proteins involved in biological pathways related to metastasis (6). Analysis of whole-cell lysates (WCL), cell surface proteins, and conditioned media identified novel proteins associated with EMT and provides evidence of a complex network of proteins regulating TGF β . Reverted cells locked in an epithelial state as a result of restoration of miR-200 displayed changes in a multitude of extracellular matrix (ECM) and cell adhesion proteins, suggesting miR-200 alters the microenvironment and the way in which cells interact with it.

Materials and Methods

Culture and isotopic labeling of cells

Parental wild-type cell lines (393P and 344SQ) derived from lung adenocarcinomas in Kras^{G12D}/p53^{R172H Δ G} mice and their derivatives stably expressing a control vector or vector with the miR-200B-200A-429 locus (344SQ_vector and 344SQ_200B) have been previously described (Gibbons, G&D). The cells were cultured in RPMI media (AthenaES) containing 10% dialyzed FBS (Gibco) and ¹³C-L-lysine or ¹³C-L-lysine and ¹³C-L-arginine (Cambridge Isotope Laboratories) instead of the unlabeled amino acids, for 7 to 8 passages as previously described (9). The same batch of cells was used for preparation of whole-cell lysates, conditioned media, and extraction of cell surface proteins. The secreted proteins were obtained by gently washing the cells 3 to 4 times in PBS prior to addition of media without FBS, followed by growth for 24 hours. During this time, cell viability was confirmed by microscopic observation and cell counting after trypan blue staining. The conditioned media were harvested; and cell debris removed by centrifugation at 5,000 \times g for 10 minutes followed by filtration through a 0.22 μ m filter. Total cell lysates were obtained by gently washing approximately 2 \times 10⁷ cells with PBS, followed by harvesting them in 1 mL (per plate) of PBS containing 1% (w/v) octyl-glucoside (OG) and protease inhibitors (complete protease inhibitor cocktail; Roche Diagnostics).

Tumors

Syngeneic tumors from the wild-type 393P and 344SQ cells (3 of each tumor type) were generated by subcutaneous injection as previously described (6). At necropsy, the tumors were flash frozen in liquid nitrogen and stored at -80°C until subsequent processing for RNA or protein. For liquid chromatography/tandem mass spectrometry (LC/MS-MS) analysis, tumors were homogenized on liquid nitrogen and lysed in 8 mol/L urea and 1% OG in 0.1 mol/L Tris-HCl at 2 mL/g of tumor.

Isolation of cell surface proteins

Cell surface proteins from the 4 cell lines, differentially labeled with heavy or light amino acids, approximately 2 \times 10⁸ of each, were biotinylated in the culture plate after gentle washing 5 times with PBS. After a 10-minute biotinyla-

tion reaction with 10 mL (per plate) of 0.25 mg/mL Sulfo-NHS-SS-Biotin in PBS at room temperature, the reaction was quenched with 15 mL of 10 mmol/L lysine in PBS. Protein was extracted in 1 mL (per plate) of PBS containing 2% NP-40 and complete protease inhibitor cocktail. Biotinylated proteins were isolated by affinity chromatography with 1 mL of Ultra-Link Immobilized Neutravidin (Pierce). Proteins bound to the column were recovered by overnight incubation with a solution of 2% OG and 1 mg/mL dithiothreitol in 0.1 mol/L Tris-HCl.

Fractionation and mass spectrometry of samples

See Supplementary methods.

Data analysis

Enrichment analysis for Gene Ontology terms was conducted on the differentially expressed proteins by Database for Annotation, Visualization, and Integrated Discovery (DAVID; refs. 10, 11). A 5-fold increase in protein enrichment in the media compared with the whole-cell lysates was used as a cutoff to identify proteins that were likely to be secreted or shed, whereas a 2-fold increase in proteins of the cell surface compared with whole-cell lysate was established for cell surface proteins. The TGF β interacting networks were generated through the use of Ingenuity Pathway Analysis (IPA; Ingenuity Systems). Protein interaction network analysis used the entire set of human protein-protein interactions cataloged in Entrez Gene (downloaded July 2009). Homologene was used to map between mouse genes and human orthologs. Graphical visualization of networks was generated using Cytoscape (12).

Western blot analysis

Cell lysates were prepared by extracting protein with RIPA buffer. For conditioned media, cells were grown for 48 hours in RPMI 1640 with 0.1% FBS, media removed, centrifuged, and filtered through a 0.22 μ m filter. Membranes were blocked in 5% nonfat dried milk and incubated overnight at 4°C with appropriate primary antibodies [PDLIM5 (Novus Biologicals), CSRP2 and ETS-1 (Santa Cruz Biotechnology), β -actin (Sigma-Aldrich), glyceraldehyde-3-phosphate dehydrogenase (Abcam), CDH1 (BD Biosciences)].

Results

Protein and mRNA profiles of metastatic and nonmetastatic tumors

We first carried out a comparative proteomic analysis of 344SQ (metastatic) and 393P (nonmetastatic) tumors described previously in Gibbons and colleagues (3 tumors of each type; refs. 6, 7). Tumor lysates were reciprocally labeled with both heavy and light acrylamide, allowing for comparisons of independent heavy/light and light/heavy metastatic versus nonmetastatic tumors, followed by reverse-phase fractionation of lysate proteins and LC-MS/MS analysis of peptide digests from each fraction (9). A total of 1,261 proteins were quantified in both reciprocally labeled experiments, of which 80 had increased ratios in metastatic versus nonmetastatic and 59 had decreased ratios at a threshold of more than 1.5-fold change in both labelings (Supplementary Table S1A and

S1B). Among the most highly enriched Gene Ontology categories for the proteins upregulated in metastatic tumors were "response to wounding, growth factor binding, calcium metal binding, and extracellular space," whereas downregulated proteins were enriched for "antigen processing and presentation and plasma membrane." We observed upregulation of multiple markers associated with mesenchymal cell function or recruit-

ment including CD73, PLAUR, clusterin, fibulin 2, integrin alpha-2, CXCL7, IGFBP3, and LTBP1. We further identified multiple proteins that have not previously been shown to play a role in metastasis including cell adhesion proteins LGALS2 and LRG1 and chitinase CHI3L4.

We next compared the proteomic findings with mRNA expression data previously obtained for the same tumors

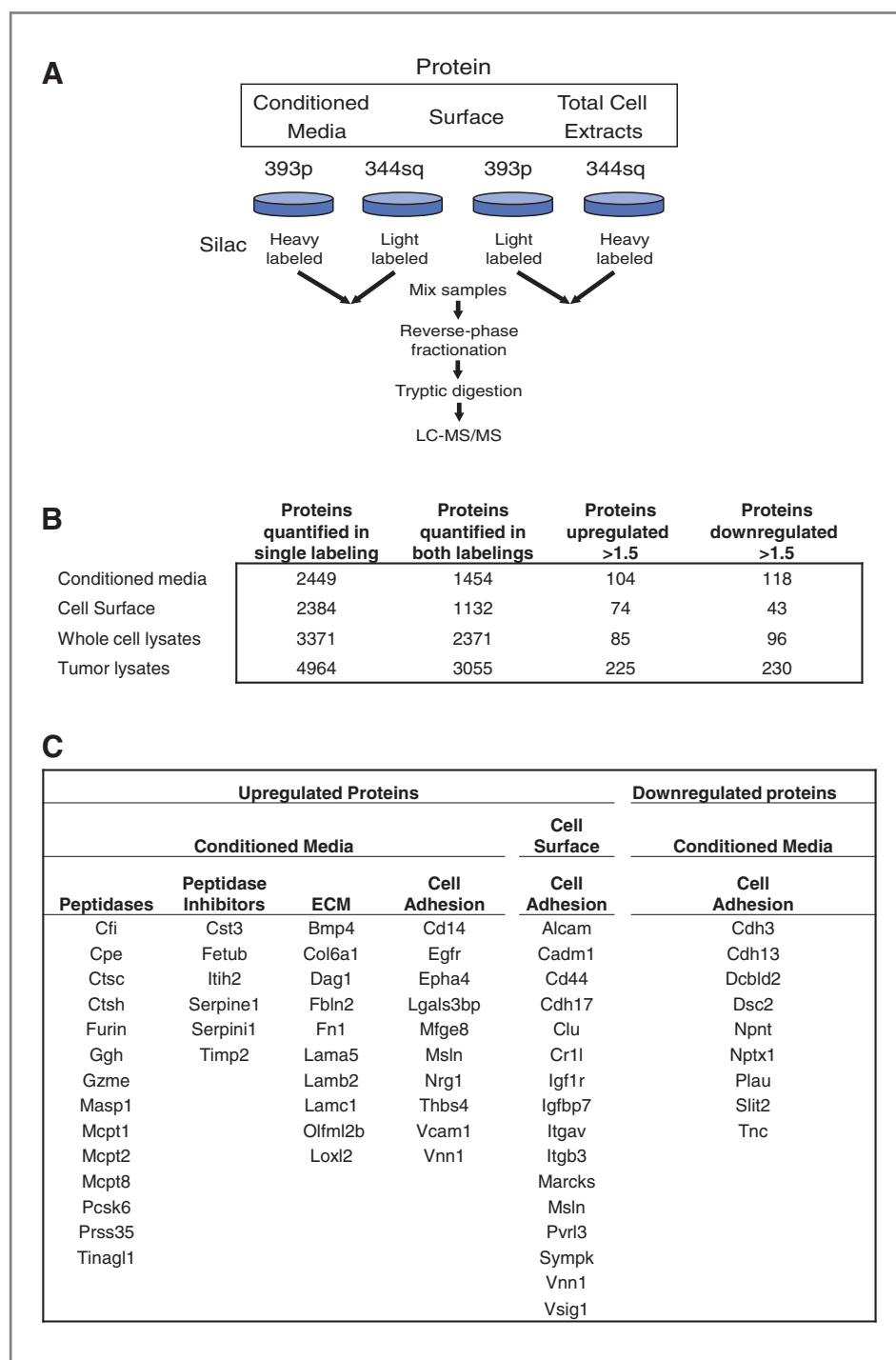


Figure 1. Protein quantifications and cellular localization. A, overview of the experimental design for mass spectrometry analysis of conditioned media, cell surface proteins, and whole-cell lysate. B, the number of identified or quantified proteins in each analysis. C, differentially regulated proteins related to the microenvironment and cellular interaction with it.

(6). Overall, there was significant positive correlation between mRNA and protein expression in tumors for both upregulated ($P = 3.80E-12$) and downregulated ($P = 8.03E-12$) proteins. However, a large number of the differentially expressed proteins were not concordantly expressed at the transcript and protein levels, notably including insulin growth factor binding proteins 3, 4, and 7, clusterin, nucleophosmin, fetuin A, and fibrinogens A and B.

Differential protein expression in metastatic and nonmetastatic cell lines

To gain a deeper understanding of the contribution of cell surface and extracellular proteins to metastasis, we conducted an in-depth proteomic analysis comparing conditioned media, cell surface proteins, and whole-cell lysates of metastatic (344SQ) and nonmetastatic (393P) cell lines. Comparative analysis was conducted with reciprocal stable isotope labeling

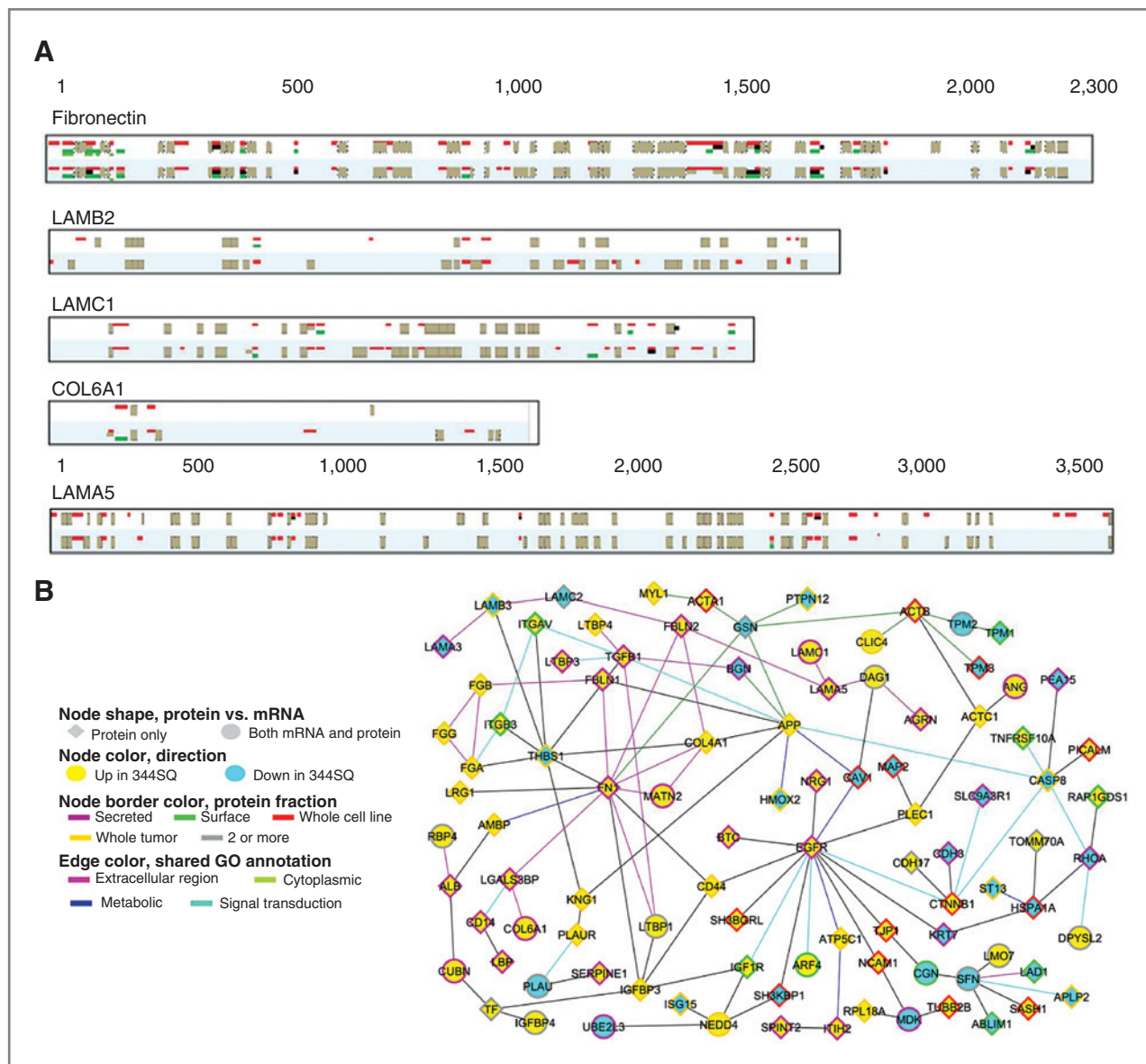


Figure 2. A, peptide coverage of ECM proteins. Peptides upregulated in 344sq are red, downregulated peptides green, unchanged peptides black, and nonquantified peptides gray. For each protein, the top is labeling mix 1 and the bottom is mix 2. B, protein-protein interaction network of differentially expressed proteins and genes (mRNAs) in 344SQ cells. Graph is comprised of proteins differentially expressed in any one of the 4 fractions (fold change >1.5, both duplicates). Nodes, proteins; circle nodes, proteins also differentially expressed at mRNA transcript level ($P < 0.01$, t test); yellow/blue, overexpression/underexpression in 344SQ, respectively. A line between 2 nodes signifies that the corresponding proteins can physically interact (according to the literature). Node border color, protein fraction showing differential patterns. Colored edges (other than gray), a common Gene Ontology term annotation shared by both of the connected proteins. GO, Gene Ontology.

by amino acids in cell culture (SILAC), whereby each cell line was grown in both heavy (^{13}C -lysine or ^{13}C -lysine + ^{13}C -arginine) and light media (allowing for comparisons of independent heavy/light and light/heavy experiments), followed by reverse-phase fractionation of samples and LC-MS/MS protein analysis (9; Fig. 1A). To identify proteins differentially regulated between the metastatic and nonmetastatic cell lines, we established a threshold of more than 1.5-fold change in both of the heavy and light SILAC labeling experiments to eliminate preferential labeling bias or contamination from trace FBS in the media (Fig. 1B, Supplementary Tables S2A and S2B). Proteins (656, 543, and 1,299) unique to each compartment were identified in the conditioned media, cell surface, and whole-cell lysate, respectively. Analysis of all 225 upregulated proteins in the metastatic cells revealed Gene Ontology functions associated with immune and inflammatory response, cell adhesion, ECM, and protease activity (Supplementary Table S3). An increase in the percentage of plasma membrane proteins found in the conditioned media was also observed, indicative of increased protein shedding from the cell surface. The Gene Ontology categories for proteins downregulated in the 344SQ cells were primarily associated with cytoskeletal regulation, cell-cell adhesion, and RNA processing. Overall, substantial changes were observed in the secreted and surface protein fractions, pertaining to components of the cellular microenvironment including ECM components, peptidase and peptidase inhibitor activities, and to proteins mediating cellular interactions with the microenvironment (Fig. 1C). Peptidases consisting of

mast cell proteases MCPT-1, 2, and 8, CFI, PCSK6, and PRSS35 were among the top 10 most highly upregulated proteins in the conditioned media of metastatic cells. Interestingly, cell adhesion molecules were also enriched by Gene Ontology analysis among both the up- and downregulated proteins in the conditioned media and the upregulated proteins on the cell surface. Differentially upregulated proteins in the whole-cell lysates were primarily associated with metabolic processes, particularly glutathione metabolism and oxidoreductase activity with upregulation of 5 glutathione-S-transferases (GST): A2, A4, M1, M2, and M7 in the whole-cell lysates of 344SQ cells, whereas downregulated proteins are enriched for cytoskeletal and actin-related proteins.

ECM proteins COL6A1, LAMA5, LAMB2, LAMC2, and fibronectin were all upregulated in 344SQ cells as well as ECM-related proteins LOXL2 which has been shown to stiffen ECM. Peptide analysis of the structural proteins COL6A1, LAMA5, LAMB2, LAMC2, and fibronectin revealed secretion of whole proteins, rather than protein fragments produced by proteolysis, providing evidence in support of tumor cells shaping their own microenvironment (Fig. 2A). Upregulation of intact fibronectin in the 344SQ metastatic cells was accompanied by downregulation of an N-terminal fragment that contains the domains for fibrinogen and collagen binding and inhibits fibronectin fibril formation (13).

Overall, substantial concordance was observed between protein expression in cell lines and tumors with respect to metastatic status, with 17 and 16 upregulated or

Table 1. Overlap between differentially regulated proteins in tumor lysates and cell lines: proteins upregulated in metastatic 344SQ tumors

Protein	Protein				mRNA	
	Conditioned media	Cell surface	Whole-cell lysates	Tumor lysates	Ratio	P
Acat1	NA	1.79	1.90	1.80	1.59	4.4E-03
Anxa10	NA	NA	2.39	5.54	16.10	5.1E-05
Cdh17	NC	2.73	NC	1.99	0.98	9.5E-01
Ckb	▲	NA	2.73	2.47	2.78	7.3E-03
Clu	8.70	5.18	2.47	4.84	1.17	5.3E-02
Fbln2	7.16	NC	2.14	2.03	0.54	9.4E-03
Igfbp4	2.14	NA	▼	2.15	1.23	5.9E-04
Igfbp7	12.92	5.10	8.97	3.02	1.23	1.4E-02
LOC677317	▲	NA	2.56	2.71	1.59	1.3E-01
Mcpt2	34.61	NA	NA	3.29	5.86	6.2E-04
Msln	3.97	12.10	2.94	1.98	1.44	7.1E-03
Nt5e	NA	NA	3.09	3.61	2.26	6.3E-04
Procr	▲	▲	3.29	2.74	1.24	3.2E-01
Pxdn	3.58	NA	NA	3.27	1.54	1.9E-02
Rbp4	3.62	NA	NA	3.04	7.49	4.3E-05
Sftpb	18.59	13.68	8.48	4.39	46.29	3.1E-05
Tspan8	NC	NC	3.46	3.22	2.56	2.6E-03

NOTE: Values are weighted means of independent and reciprocally labeled replicates. Proteins up- or downregulated, but less than 1.5 are indicated by "▲" or "▼." "NC" indicates the replicates are not concordant. "NA" indicates the protein was not quantified.

downregulated in common, respectively, and only 3 proteins with discordant findings between the 2 data sets (Tables 1 and 2). The concordance observed between the cell lines and tumors is indicative of the contribution of tumor cells to the tumor proteome. Moreover, we observed significant correlation between tumor mRNA expression and proteins in the conditioned media ($P = 3.80E-12$ for upregulated and $8.03E-12$ for downregulated proteins), cell surface ($P = 2.29E-08$ for upregulated and $3.01E-09$ for downregulated proteins), and whole-cell lysates ($P = 4.67E-16$ for upregulated and $5.80E-21$ for downregulated proteins). As a tool for better understanding and illustrating the comparison and complementation of the protein and mRNA changes, we integrated our top differential proteins with the public Entrez Gene database of protein-protein interactions to generate a protein interaction network, in which we labeled those proteins showing corresponding differential changes at the mRNA level (Fig. 2B).

Protein components of the TGF β network in metastatic tumors and cell line compartments

We next used IPA tools to identify potential regulatory pathways accounting for the differences between the metastatic and nonmetastatic cells. Analysis of differentially regulated proteins from the conditioned media, cell surface, and whole-cell lysates revealed regulatory nodes associated with NF- κ B, fibronectin, and p38 mitogen-activated protein kinase (Supplementary Fig. S1). Networks with TGF β -1 were also identified in the individual compartments, par-

ticularly the conditioned media (Fig. 3A, see Supplementary Fig. S2 for TGF β containing networks from all subproteomes). However, analysis of the combined upregulated proteins by IPA identified TGF β -1 as the central regulatory node in the most highly significant network, with an IPA significance score of 64 versus 33 for the second network generated (Fig. 3B). This finding highlights the power of data synthesis from multiple cellular compartments to enhance the ability to find master regulators, as TGF β -1 was identified as one of several regulatory proteins in the individual analyses but was shown to be the dominant regulator in the analysis of combined protein compartments. Furthermore, we observed evidence of a multilayer regulation of TGF β -1 in the differential expression of TGF β -1 regulatory proteins. Proteases PCSK6 (also known as PACE4) and FURIN activate TGF β -1 through proteolytic cleavage, TGF β latency complex protein LTBP3, and integrins α V and β 3, which have been shown to be involved in TGF β -1 activation, were all upregulated in 344SQ cells whereas the TGF β latency complex protein, LTBP1 and the TGF β -1 binding proteins BGN were downregulated (Fig. 3C; refs. 14, 15). We further identified isoform differences in the latent transforming growth factor binding proteins (LTBP). An N-terminal peptide corresponding to cleavage at the LTBP3 hinge region which elutes out earlier by reverse-phase high-performance liquid chromatography is reduced in metastatic 344SQ cells, whereas there is upregulation of the full-length protein. The LTBP1 proteins are downregulated in 344SQ cells and also show

Table 2. Overlap between differentially regulated proteins in tumor lysates and cell lines: proteins downregulated in metastatic 344SQ tumors

Protein	Protein				mRNA	
	Conditioned media	Cell surface	Whole-cell lysates	Tumor lysates	Ratio	P
Anxa6	▲	NC	0.59	0.58	0.49	4.9E-03
Cald1	▼	0.43	NC	0.56	0.85	7.8E-01
Capg	▼	NA	0.52	0.37	0.55	3.1E-03
Cda	NA	▼	0.31	0.42	0.45	3.2E-06
Crip1	0.57	NC	NC	0.44	0.84	3.0E-02
H2-K1	0.41	NA	NA	0.42	0.72	1.3E-01
Ifi204	NA	0.56	0.21	0.28	0.89	6.3E-01
Lamc2	▼	0.50	NA	0.27	0.81	7.3E-02
Ly6a	0.20	NA	0.23	0.33	0.42	3.8E-03
Raly	NA	NA	0.39	0.39	0.67	1.5E-02
S100a14	NA	0.30	0.15	0.09	0.01	4.9E-08
Sfn	▼	NC	0.28	0.10	0.44	8.6E-04
Sh3bgrl2	0.44	NA	0.43	0.64	1.00	9.8E-01
Tacstd1	NC	NC	0.15	0.21	0.08	1.7E-04
Uchl1	NA	NA	0.25	0.53	0.82	3.0E-01
Zyx	0.53	NA	NC	0.61	0.51	2.9E-04

NOTE: Values are weighted means of independent and reciprocally labeled replicates. Proteins up- or downregulated, but less than 1.5 are indicated by "▲" or "▼." "NC" indicates the replicates are not concordant. "NA" indicates the protein was not quantified.

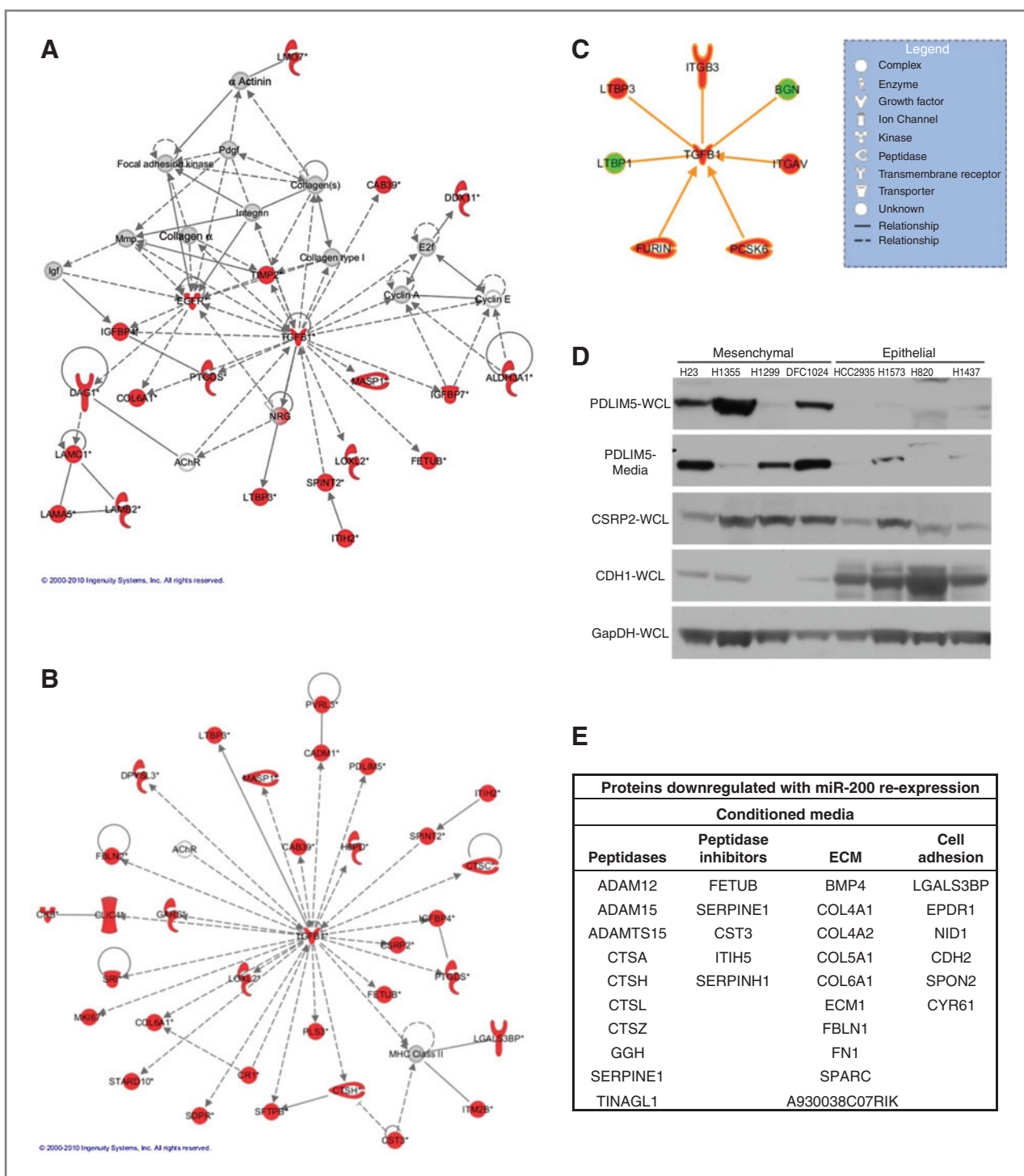


Figure 3. TGFβ signaling in metastatic cells. A, the most significant network from IPA for upregulated proteins in the conditioned media shows evidence of TGFβ-1 regulation. B, network analysis of upregulated proteins combined from conditioned media, cell surface, and total cell extracts reveals a stronger and more significant node than from the individual compartments. C, proteins directly interacting with and regulating TGFβ-1. Network objects colored red indicate upregulation and green objects indicate downregulation. D, Western blots comparing protein expression in epithelial and mesenchymal NSCLC cell lines. E, microenvironment-related proteins downregulated with miR-200 expression.

downregulation likely of an N-terminal product, although it is larger than the cleavage product resulting from processing of LTBP1 at the hinge region (16).

Identification of novel metastasis-associated proteins

Integrated data analysis of lysate, conditioned media, and cell surface components for proteins associated with

Table 3. miR-200 regulation of proteins

Genes	Protein		mRNA			
	344SQ/393P	344SQ_miR-200/344SQ_control	344SQ/393P		344SQ_miR-200/ 344SQ_control	
	Ratio	Ratio	Ratio	P	Ratio	P
<i>B4galt5</i>	4.60	0.39	1.20	3.35E-01	1.29	1.48E-01
<i>Bmp4</i>	2.90	0.43	4.88	5.13E-03	0.17	7.89E-03
<i>Col6a1</i>	3.47	0.57	1.97	3.98E-03	0.71	6.40E-02
<i>Cst3</i>	1.76	0.49	1.05	5.39E-01	0.46	2.79E-04
<i>Ctsc</i>	3.74	0.48	1.27	2.83E-01	1.23	2.79E-01
<i>Ctsh</i>	5.36	0.28	1.83	9.79E-03	0.26	1.15E-02
<i>Egfr</i>	2.84	0.39	1.24	5.72E-02	1.16	5.88E-02
<i>Fetub</i>	2.98	0.47	0.87	3.34E-02	0.87	2.69E-01
<i>Fn1</i>	1.73	0.48	0.88	9.23E-02	2.15	7.12E-02
<i>Ggh</i>	2.91	0.59	0.69	4.85E-01	1.01	9.24E-01
<i>Gnptg</i>	2.26	0.39	1.09	5.20E-01	0.78	2.70E-01
<i>Lgals3bp</i>	6.52	0.42	1.88	1.04E-02	0.20	2.26E-03
<i>Loxl2</i>	4.34	0.36	0.87	7.84E-01	0.67	1.77E-01
<i>Man2b1</i>	2.59	0.44	0.92	2.46E-01	1.04	4.62E-01
<i>Manba</i>	2.67	0.39	1.20	3.73E-01	0.59	2.39E-01
<i>Mcpt2</i>	34.61	0.10	5.86	6.16E-04	0.01	6.88E-05
<i>Mcpt8</i>	12.11	0.58	3.97	2.22E-03	0.64	8.32E-02
<i>Mfge8</i>	5.06	0.61	0.99	5.92E-01	0.86	4.23E-01
<i>Prl2c4</i>	2.60	0.25	0.37	2.57E-02	0.36	3.29E-02
<i>Serpine1</i>	6.95	0.25	1.13	1.09E-01	0.68	3.56E-01
<i>Sftpb</i>	18.59	0.08	46.29	3.10E-05	0.02	1.06E-05
<i>Tinagl1</i>	4.04	0.52	1.24	2.09E-02	0.89	2.43E-01

NOTE: Overlap between proteins upregulated in 344SQ cells and downregulated after re-expression of miR-200. Values for proteins are weighted averages of reciprocal labeling experiments.

metastasis yielded several novel proteins. LRRC8 is a known endoplasmic reticulum protein which we found to be upregulated on the surface of metastatic cells. Cytoskeletal protein PDLIM5 was also upregulated on the surface of metastatic cells and showed evidence of cleavage, with the first half and the second half of the protein eluting out in different fractions. Another lim-containing protein, CSR2, was upregulated and occurred as an intact protein in the cell surface fraction. Many novel secreted proteins were also upregulated. Fibulin 2, previously suggested to be a tumor suppressor was upregulated 7-fold, MASP1 and peroxidase were upregulated 3-fold. In addition, several cytoplasmic and nuclear proteins were found to be secreted by metastatic cells including ST3GAL4, ST6GAL1, SIL1, and SDF4. Expression of several proteins upregulated in 344SQ cells was evaluated in human non-small cell lung cancer cell lines (NSCLC) with mesenchymal or epithelial features. CSR2 and PDLIM5 were expressed at higher levels in cells with mesenchymal features than more epithelial cell lines. PDLIM5 was further upregulated in conditioned media from mesenchymal NSCLC cell lines (Fig. 3D). These findings show the applicability of findings in the mouse model to human lung cancer.

Identification of miR-200-regulated proteins

miR-200 regulates EMT and metastasis at least, in part, through a negative regulatory loop with the Zeb1/2 family of transcriptional repressors (6, 17). As one of the primary biological differences between the metastatic 344SQ cells and the nonmetastatic 393P cells is the expression of the miR-200 family members, we investigated the effect of miR-200 on protein expression. For this analysis, 344SQ cell lines (which normally have low miR-200 expression) with stable miR200b-200a-429 (344SQ_miR-200) expression or a vector control (344SQ_vector) were established and their protein constituents analyzed by LC/MS-MS. We identified 193 upregulated proteins and 179 downregulated proteins in the combined subproteomes in 344SQ_miR-200 cells (Supplementary Tables S4A, S4B, and S4C). Gene Ontology analysis of differentially regulated proteins revealed similar findings to the 344SQ/393P analysis, as categories associated with peptidase activity, cell adhesion, and ECM among the proteins downregulated with miR-200 restoration, whereas proteins upregulated with miR-200 restoration were associated primarily with cytoskeletal regulation and cell adhesion (Supplementary Tables S5).

Table 4. Protein and gene expression correlation with miR-200 family members in human NSCLC cell lines

Conditioned media	344SQ_ miR-200/ 344SQ_ control Protein ratio	Protein					mRNA				
		miR-200a	miR-200b	miR-429	miR-200c	miR-141	miR-200a	miR-200b	miR-429	miR-200c	miR-141
CDH1	1.67	0.59	0.56	0.37	0.7	0.7	0.71	0.74	0.7	0.92	0.92
EPS8L2	2.05	0.53	0.56	0.39	0.59	0.63	0.56	0.51	0.44	0.22	0.22
IRF2BP2	3.07	0.14	0.41	0.36	0.18	0.16	0.34	0.46	0.39	0.4	0.42
KRT7	2.52	0.63	0.59	0.53	0.53	0.55	0.55	0.52	0.48	0.49	0.48
KRT8	1.78	0.23	0.49	0.27	0.44	0.49	0.32	0.31	0.26	0.48	0.46
KRT19	2.24	0.6	0.59	0.45	0.58	0.59	0.65	0.59	0.52	0.76	0.76
Cell surface											
Atp1b1	1.65	0.39	0.45	0.45	0.39	0.42	0.4	0.44	0.38	0.5	0.5
F3	1.64	0.49	0.45	0.32	0.42	0.4	0.67	0.66	0.61	0.57	0.56
F11R	1.71	0.35	0.44	0.24	0.31	0.34	0.54	0.61	0.57	0.57	0.58
LSR	1.57	0.45	0.43	0.42	0.43	0.4	0.42	0.38	0.35	0.53	0.53
SDCBP2	1.89	0.38	0.3	0.21	0.41	0.42	0.6	0.62	0.5	0.62	0.63
Whole-cell lysate											
EPS8L2	1.65	0.55	0.57	0.37	0.57	0.58	0.56	0.51	0.44	0.22	0.22
GOLGA2	1.63	0.35	0.26	0.26	0.44	0.4	0.39	0.44	0.38	0.59	0.59
PLS1	1.60	0.44	0.55	0.36	0.44	0.46	0.63	0.62	0.62	0.5	0.49

NOTE: Spearman and Pearson correlation coefficients are listed for protein and mRNA expression, respectively, with r values having a $P < 0.01$ in bold.

Restoration of miR-200 expression affects the microenvironment through protein shedding and secretion

To ascertain changes in cellular functions after restoration of miR-200 expression, we assessed the differentially regulated proteins from conditioned media, cell surface, and whole-cell lysates. The most striking effect of miR-200 expression was a change in protein constituents in the media resulting from protein secretion and shedding with downregulation of ECM, peptidases, and cell adhesion proteins in the conditioned media from the 344SQ_miR-200 cells (Fig. 3E). Twenty-two proteins upregulated in the 344SQ/393P conditioned media were downregulated in conditioned media from 344SQ_miR-200 cells, suggesting direct regulation by miR-200 (Table 3). Furthermore, there was significant correlation between protein and mRNA expression in the downregulated proteins from the 344SQ_miR-200/vector control comparison ($P = 6.38E-12$), supporting the role miR-200 plays in altering the cellular microenvironment. To validate proteins regulated by miR-200, we analyzed expression of proteins downregulated after miR-200 expression in 344SQ cells in a set of human NSCLC cell lines for which we have miRNA expression data. Several proteins in each compartment correlated with miR-200 family expression at both the RNA and protein level in NSCLC human cell lines (Table 4), including known miR-200 targets such as CDH1, but also EPS8L2, PLS1, LSR, and others.

We have previously shown that miR-200 expression alters many genes at the expression level through an indirect effect. Though restoring miR-200 expression in 344SQ cells reverted the EMT, the small number of overlapping proteins upregulated in 344SQ cells and downregulated after miR-200 expression is restored suggests the occurrence of regulatory mechanisms other than direct inhibition of miR-200. To elucidate alternative mechanisms for regulation of genes associated with EMT, the publicly available software package Amadeus was used to search for common DNA motifs in promoter sequences from differentially regulated genes (Supplementary Table S6; ref. 18). One transcription factor identified in upregulated proteins is the oncogene *C-ets-1*, a member of the ETS family that has been shown to be upregulated in invasive cancers and to be an effector of TGF β -induced EMT, by upregulating *Zeb1* (19, 20). ZEB1 DNA binding elements were enriched in both the downregulated mRNA and protein data sets (Supplementary Table S7). *Zeb1* is a validated target of miR-200 that was previously shown to be upregulated in 344SQ cells, whereas *C-ets-1* was recently shown to be a direct miR-200 target in human endothelial cells. Expression of *C-ets-1* was regulated by miR-200 at both the mRNA and protein level (Fig. 4A and B). Activity of a luciferase reporter containing the 3' untranslated region (UTR) for *C-ets-1* was directly regulated by cotransfection of miR-200B and C, but not miR-200A, as predicted from the seed sequence sites found in the 3' UTR (Fig. 4C and D).

This is in contrast to the 3' UTR for *Zeb1*, which has documented sites for both of the miR-200 family seed sequences. Another transcription factor, AP-2REP, was also identified in both the downregulated mRNA and protein data sets and has been shown to be amplified in invasive gastric cancer and salivary tumors (21). Activating transcription factors, known to mediate and regulate effects of TGF β , were also enriched in the upregulated mRNAs. Interestingly, binding sites for ETS2, which shares overlapping function with ETS1 during mouse development, were identified in the downregulated mRNA, suggesting differential roles for ETS1 and ETS2 during tumor progression, a finding supported by transcript analysis in human lung cancer cell lines (data not shown).

Discussion

In this work, we have carried out an in-depth systems analysis of metastatic lung tumors which spontaneously undergo EMT, identifying changes in the deposition of ECM, protease function,

and cell adhesion. Although prior studies of EMT using proteomics have been primarily based on total lysates from cancer cell lines, we expanded on previous findings with analysis of tumors and subproteomes from primary cell lines (22–24). Our initial proteomic analysis comparing metastatic and nonmetastasizing primary cell lines grown as syngeneic murine tumors revealed a large number of proteins (80 up and 59 down) potentially involved in tumor progression, whereas analysis by LC/MS-MS of cultured cell lines labeled *in vitro* enabled protein identification and quantitation of intracellular, cell surface, and secreted/shed proteins, greatly increasing the total number of differentially regulated proteins and providing insight into protein processing. Integration of data from the subproteomes enabled identification of relevant biological functions such as changes in ECM and cell adhesion and pertinent regulatory networks, notably regulators of the metastatic driver TGF β -1. Findings included increased expression of the proteolytic activators FURIN and PCSK6 in the conditioned media, as well as differential regulation of latent transforming binding proteins.

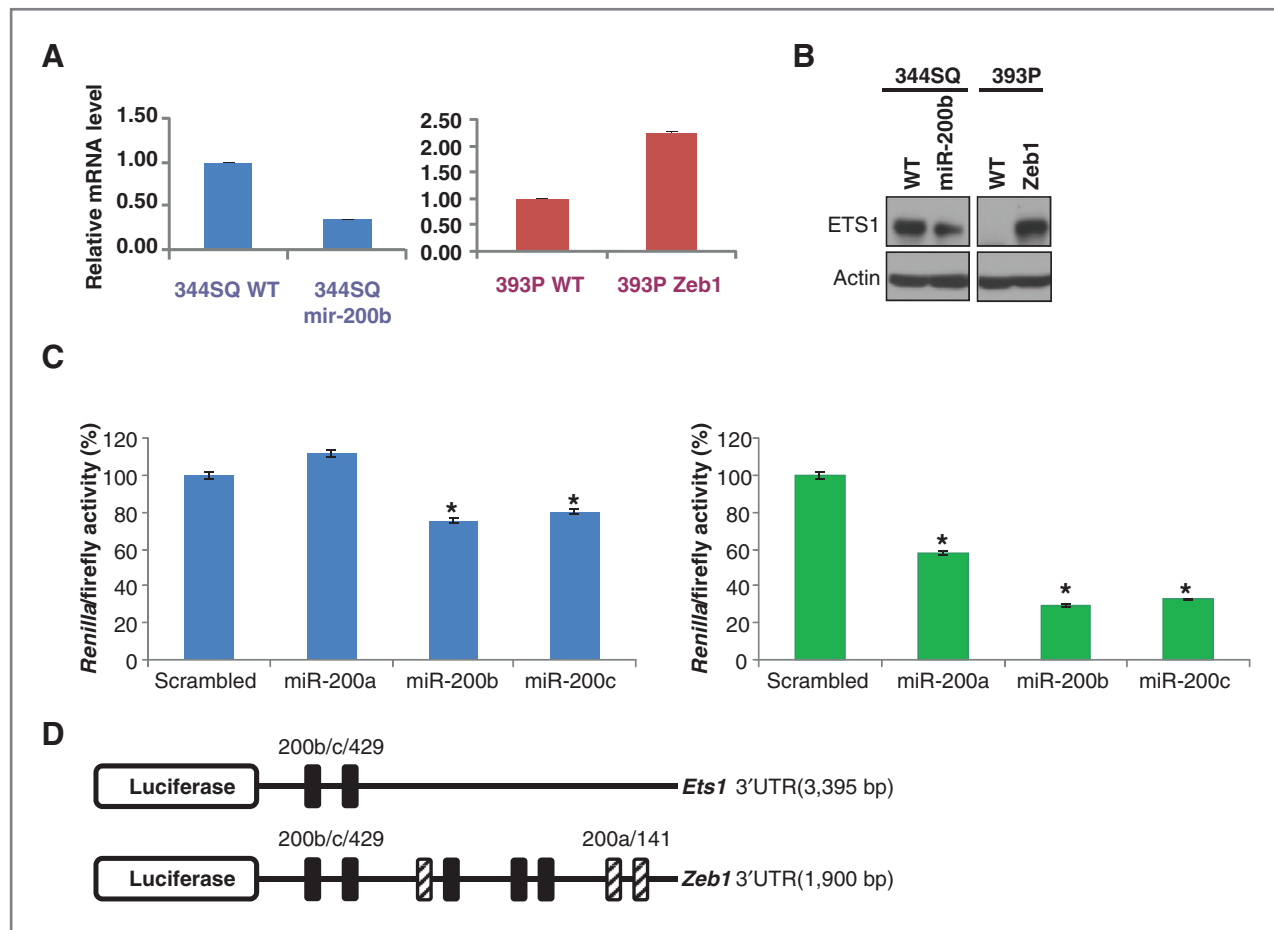


Figure 4. ETS-1 regulation by miR-200. **A**, quantitative real-time PCR analysis of ETS-1 mRNA levels in 344SQ or 393P cells stably transfected with an empty vector control (WT), the miR-200b/a/429 locus (200b), or Zeb1 normalized on the basis of L32 ribosomal protein mRNA levels and expressed as mean values of triplicate cultures relative to control transfectants, which were set at 1.0. **B**, Western blot analysis of the same cell lines. **C**, 344SQ cells were transiently cotransfected with the indicated pre-miRs or scrambled oligomer (10 nmol/L) and reporter plasmids (500 ng) that are linked to the full-length 3'-UTR of *ETS-1* (left) or *Zeb1* (right). Results were normalized on the basis of *Renilla* luciferase and expressed as the mean values of triplicate wells. *, $P < 0.05$. **D**, map of 3' UTR for luciferase assays showing miR-200 target sites.

ECM regulation of cell behavior is transmitted through cell surface receptors, embedded cytokines and growth, as well as by posttranslational modification and matrix stiffness. Numerous changes were observed in ECM proteins, proteases, and cell adhesion in the metastatic 344SQ cells, including upregulation of full-length lamins A5, B2, and C1, collagen 6A1, fibronectin, Loxl2, a protein involved in the stiffening of collagen, and biglycan, a collagen binding partner. Although the classical model of tumor progression includes degradation of the ECM for cells to invade through the basement membrane, we observed increased production of particular full-length ECM proteins without evidence of degradation. These effects are in part driven by miR-200 expression as there was significant downregulation of ECM proteins after miR-200 reexpression. Interestingly, although there was an increase in laminins (laminin $\alpha 5$, $\beta 2$, and $\gamma 1$) secreted by the 344SQ cells, collagens (collagens 4A1, 4A2, 5A1, and 6A1) were the primary ECM structural component reduced with miR-200 restoration. Increased ECM production has been observed in several cancer types, such as oral squamous cell carcinomas, colorectal cancer, and breast cancer (25, 26). The apparent switch from laminins to collagens, along with expression of fibronectin and lysyl oxidase homolog 2, stiffens the matrix, a finding which has been shown to aid in tumor progression in several tumor models, but not so far in lung cancer (reviewed in ref. 27). This downregulation of collagens and matrix stiffening proteins with miR-200 expression implies a specific novel role for miR-200 in collagen production. Other miRNAs have previously been shown to play

roles in fibrosis through regulation of ECM proteins; miR-29 family members downregulate collagens and fibrillins in hepatic and cardiac fibroblasts, whereas miR-21 mediates pulmonary fibrosis, but this is the first evidence of miRNA effects on the microenvironment during tumorigenesis (28, 29). Recent work by Korpala and colleagues identified Sec23a as an miR-200 target important for mediating the secretion of metastasis-related proteins in breast cancer cell line (30). Many of the proteins they identified as being miR-200- or Sec23a dependent were also identified in our study, such as IGFBP4, Tinagl1, and Ltbp3, although the total number of differentially regulated proteins in our study was more, likely due to the higher resolution provided by more extensive fractionation. Sec23a itself was upregulated in the mRNA expression analysis, but only in one of the two 344SQ/393P proteomic analyses, not meeting our stringent threshold for upregulation.

In addition to ECM structural proteins, we also observed differential regulation of peptidases and cell adhesion proteins in 344SQ cells and downregulation of peptidases with miR-200 restoration. Of the 22 proteins in the 344SQ/393P conditioned media that seem to be directly regulated by miR-200, 8 were peptidases or peptidase inhibitors. Expression and processing of cell adhesion molecules were also modified in 344SQ cells and closer investigation of the specific cellular adhesion proteins reveals a shift from proteins functioning in cell-cell adhesion and epithelial phenotype to cell-matrix adhesion and mesenchymal phenotype (Fig. 5). Cell surface adhesion molecules CDH17, integrins αV and $\beta 3$, and CD44, all directly bind

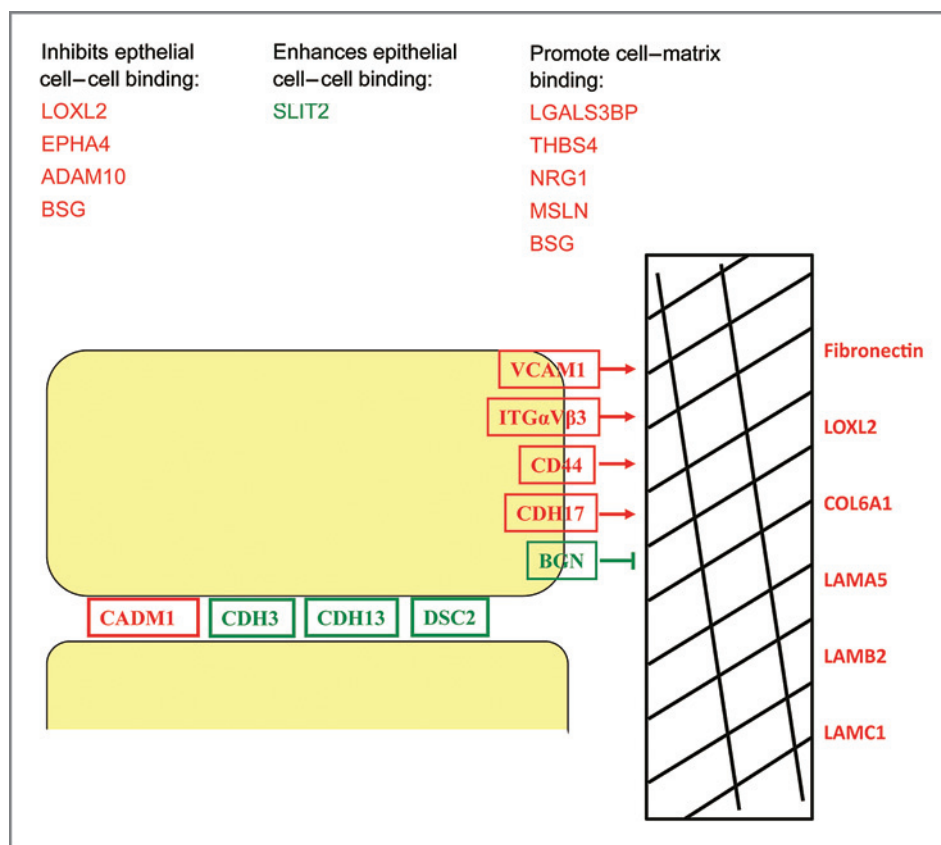


Figure 5. Regulation of cell adhesion proteins in 344SQ metastatic cells. Cell adhesion and ECM proteins are differentially regulated in metastatic cells. Changes of protein expression observed in 344SQ cells reveal enhanced binding to ECM and decreased cell-cell adhesion along with upregulation of ECM. Upregulated proteins are labeled in red and downregulated proteins in green.

cells to ECM whereas secreted LGALS3BP, neuregulin, and THBS4 increase cell-matrix adhesion (31, 32) and Adam10, Loxl2, and EPHA4 inhibit cell-cell adhesion (33–35). Adhesion proteins downregulated in the media, such as cadherins 3 and 13, desmocollin 2, and SLIT2 promote epithelial cell-cell adhesion, and loss is associated with increases in invasion and tumor progression (36–38). The changes in ECM, peptidases, and cell adhesion proteins represent remodeling of the microenvironment and the cell surface after or coincident with EMT.

In order for a tumor to progress, tumor cells must be capable of self-renewal, likely through cancer stem cells. The stem cell marker CD44 was upregulated in 344SQ cells along with mesenchymal stem cell markers CD9 and CD106 (VCAMI; refs. 39, 40). We also observed upregulation of 2 aldehyde dehydrogenases (ALDH3A1 and ALDH1A7); aldehyde dehydrogenase activity and ALDH3A1 in particular have been suggested as markers of cancer stem cells in several cancer types (41). An increase in glutathione transferase expression has also been correlated with CD133 expression in NSCLC tumor samples, and we have recently identified a metastatic subpopulation of cells in this model to be CD133+ (42). We further observe upregulation of 5 GSTs (GSTM1, GSTA2, GSTM2, GSTA4, and GSTM7) in metastatic 344SQ cells, suggesting GST activity plays an important role in metastasis and may be another potential marker for cancer stem cells. Reactive oxygen species (ROS) play a role in many aspects of metastasis, including cell adhesion, motility, cell death, and other cancer-related pathways, and glutathione scavenging of reactive species and free radicals is a mechanism by which cells prevent the damage of ROS, with GSTs catalyzing the binding of reduced glutathione to both endogenous and exogenous reactive species, reducing the toxicity of these molecules (43).

In our proteomics analysis, we observed evidence of transcriptional regulation in 8 of the 22 proteins downregulated in conditioned media after miR-200 overexpression. Furthermore, comparison of the 22 gene list with Targetscan and Pictar predicted miR-200-regulated genes reveals only 1 miR-

200 predicted gene on the list, fibronectin. We cannot ascertain from this data whether the affected genes in this list are direct targets of miR-200, but previous analysis of microRNA regulation also revealed large numbers of affected genes that do not have 3' UTR consensus sequences for miR-200 regulation (44, 45). miR-200 functions in a feedback loop with the transcriptional repressors *Zeb1* and *Zeb2* to regulate the EMT through miR-200 active sites in the 3' UTR of *Zeb*, whereas ZEB1 and ZEB2 are also capable of repressing transcription of miR-200 family members (46). ZEB1 was found to be overexpressed in metastatic 344SQ cells and may be responsible for changes in gene expression that are not accounted for by miR-200. The identification of ZEB1 binding domains in the promoters of downregulated proteins and transcripts raises the possibility that the miR-200 family's effect is a combination of direct suppression and regulation of multiple transcription factors, such as *Zeb1* and *c-ets-1*. Promoter analysis of differentially regulated genes further revealed other potential transcription factors with a role in EMT such as *Ap-2rep*. Further study is required to elucidate the combined role for these factors in EMT and metastasis.

Disclosure of Potential Conflicts of Interest

No potential conflicts of interest were disclosed.

Grant Support

This work was supported by the NCI Mouse Models of Human Cancer Consortium and NIH R01 CA157450. D.L. Gibbons was supported by a Young Investigator Award from The ASCO Cancer Foundation, an International Association for the Study of Lung Cancer (IASLC) Fellow grant, and NCI K08 CA151651. J.M. Kurie is the Elza A. and Ina Shackelford Freeman Endowed Professor in Lung Cancer. C. Ungewiss was supported by the Training Program in Molecular Genetics of Cancer, NIH/NCI T32 CA009299-32.

The costs of publication of this article were defrayed in part by the payment of page charges. This article must therefore be hereby marked *advertisement* in accordance with 18 U.S.C. Section 1734 solely to indicate this fact.

Received March 20, 2011; revised September 8, 2011; accepted September 29, 2011; published OnlineFirst October 10, 2011.

References

- Thiery JP, Acloque H, Huang RY, Nieto MA. Epithelial-mesenchymal transitions in development and disease. *Cell* 2009;139:871–90.
- Siegel PM, Shu W, Massague J. Mad upregulation and Id2 repression accompany transforming growth factor (TGF)-beta-mediated epithelial cell growth suppression. *J Biol Chem* 2003;278:35444–50.
- Huber MA, Kraut N, Beug H. Molecular requirements for epithelial-mesenchymal transition during tumor progression. *Curr Opin Cell Biol* 2005;17:548–58.
- Bracken CP, Gregory PA, Khew-Goodall Y, Goodall GJ. The role of microRNAs in metastasis and epithelial-mesenchymal transition. *Cell Mol Life Sci* 2009;66:1682–99.
- Park SM, Gaur AB, Lengyel E, Peter ME. The miR-200 family determines the epithelial phenotype of cancer cells by targeting the E-cadherin repressors ZEB1 and ZEB2. *Genes Dev* 2008;22:894–907.
- Gibbons DL, Lin W, Creighton CJ, Rizvi ZH, Gregory PA, Goodall GJ, et al. Contextual extracellular cues promote tumor cell EMT and metastasis by regulating miR-200 family expression. *Genes Dev* 2009;23:2140–51.
- Zheng S, El-Naggar AK, Kim ES, Kurie JM, Lozano G. A genetic mouse model for metastatic lung cancer with gender differences in survival. *Oncogene* 2007;26:6896–904.
- Gibbons DL, Lin W, Creighton CJ, Zheng S, Berel D, Yang Y, et al. Expression signatures of metastatic capacity in a genetic mouse model of lung adenocarcinoma. *PLoS One* 2009;4:e5401.
- Faca VM, Ventura AP, Fitzgibbon MP, Pereira-Faca SR, Pitteri SJ, Green AE, et al. Proteomic analysis of ovarian cancer cells reveals dynamic processes of protein secretion and shedding of extra-cellular domains. *PLoS One* 2008;3:e2425.
- Dennis G Jr., Sherman BT, Hosack DA, Yang J, Gao W, Lane HC, et al. DAVID: database for annotation, visualization, and integrated discovery. *Genome Biol* 2003;4:P3.
- Huang da W, Sherman BT, Lempicki RA. Systematic and integrative analysis of large gene lists using DAVID bioinformatics resources. *Nat Protoc* 2009;4:44–57.
- Shannon P, Markiel A, Ozier O, Baliga NS, Wang JT, Ramage D, et al. Cytoscape: a software environment for integrated models

- of biomolecular interaction networks. *Genome Res* 2003;13:2498–504.
13. Saulnier R, Bhardwaj B, Klassen J, Leopold D, Rahimi N, Tremblay E, et al. Fibronectin fibrils and growth factors stimulate anchorage-independent growth of a murine mammary carcinoma. *Exp Cell Res* 1996;222:360–9.
 14. Constam DB, Robertson EJ. Tissue-specific requirements for the proprotein convertase furin/SPC1 during embryonic turning and heart looping. *Development* 2000;127:245–54.
 15. Dubois CM, Laprise MH, Blanchette F, Gentry LE, Leduc R. Processing of transforming growth factor beta 1 precursor by human furin convertase. *J Biol Chem* 1995;270:10618–24.
 16. Taipale J, Miyazono K, Heldin CH, Keski-Oja J. Latent transforming growth factor-beta 1 associates to fibroblast extracellular matrix via latent TGF-beta binding protein. *J Cell Biol* 1994;124:171–81.
 17. Gregory PA, Bracken CP, Bert AG, Goodall GJ. MicroRNAs as regulators of epithelial-mesenchymal transition. *Cell Cycle* 2008;7:312–8.
 18. Linhart C, Halperin Y, Shamir R. Transcription factor and microRNA motif discovery: the Amadeus platform and a compendium of meta-zoan target sets. *Genome Res* 2008;18:1180–9.
 19. Dittmer J. The biology of the Ets1 proto-oncogene. *Mol Cancer* 2003;2:29.
 20. Koinuma D, Tsutsumi S, Kamimura N, Taniguchi H, Miyazawa K, Sunamura M, et al. Chromatin immunoprecipitation on microarray analysis of Smad2/3 binding sites reveals roles of ETS1 and TFAP2A in transforming growth factor beta signaling. *Mol Cell Biol* 2009;29:172–86.
 21. Nakamura Y, Migita T, Hosoda F, Okada N, Gotoh M, Arai Y, et al. Kruppel-like factor 12 plays a significant role in poorly differentiated gastric cancer progression. *Int J Cancer* 2009;125:1859–67.
 22. Keshamouni VG, Jagtap P, Michailidis G, Strahler JR, Kuick R, Reka AK, et al. Temporal quantitative proteomics by iTRAQ 2D-LC-MS/MS and corresponding mRNA expression analysis identify post-transcriptional modulation of actin-cytoskeleton regulators during TGF-beta-Induced epithelial-mesenchymal transition. *J Proteome Res* 2009;8:35–47.
 23. Mathias RA, Wang B, Ji H, Kapp EA, Moritz RL, Zhu HJ, et al. Secretome-based proteomic profiling of Ras-transformed MDCK cells reveals extracellular modulators of epithelial-mesenchymal transition. *J Proteome Res* 2009;8:2827–37.
 24. Zhou C, Nitschke AM, Xiong W, Zhang Q, Tang Y, Bloch M, et al. Proteomic analysis of tumor necrosis factor-alpha resistant human breast cancer cells reveals a MEK5/Erk5-mediated epithelial-mesenchymal transition phenotype. *Breast Cancer Res* 2008;10:R105.
 25. Kulasekara KK, Lukandu OM, Neppelberg E, Vintermyr OK, Johannessen AC, Costea DE. Cancer progression is associated with increased expression of basement membrane proteins in three-dimensional in vitro models of human oral cancer. *Arch Oral Biol* 2009;54:924–31.
 26. Kass L, Erler JT, Dembo M, Weaver VM. Mammary epithelial cell: influence of extracellular matrix composition and organization during development and tumorigenesis. *Int J Biochem Cell Biol* 2007;39:1987–94.
 27. Kumar S, Weaver VM. Mechanics, malignancy, and metastasis: the force journey of a tumor cell. *Cancer Metastasis Rev* 2009;28:113–27.
 28. Liu G, Friggeri A, Yang Y, Milosevic J, Ding Q, Thannickal VJ, et al. miR-21 mediates fibrogenic activation of pulmonary fibroblasts and lung fibrosis. *J Exp Med* 2010;207:1589–97.
 29. Roderburg C, Urban GW, Bettermann K, Vucur M, Zimmermann H, Schmidt S, et al. Micro-RNA profiling reveals a role for miR-29 in human and murine liver fibrosis. *Hepatology* 2011;53:209–18.
 30. Korpala M, Ell BJ, Buffa FM, Ibrahim T, Blanco MA, Celia-Terrassa T, et al. Direct targeting of Sec23a by miR-200s influences cancer cell secretome and promotes metastatic colonization. *Nat Med* 2011;17:1101–8.
 31. Ozaki Y, Kontani K, Teramoto K, Fujita T, Tezuka N, Sawai S, et al. Involvement of 90K/Mac-2 binding protein in cancer metastases by increased cellular adhesiveness in lung cancer. *Oncol Rep* 2004;12:1071–7.
 32. Dunkle ET, Zaucke F, Clegg DO. Thrombospondin-4 and matrix three-dimensionality in axon outgrowth and adhesion in the developing retina. *Exp Eye Res* 2007;84:707–17.
 33. Puschmann TB, Turnley AM. Eph receptor tyrosine kinases regulate astrocyte cytoskeletal rearrangement and focal adhesion formation. *J Neurochem* 2010;113:881–94.
 34. Schietke R, Warnecke C, Wacker I, Schodel J, Mole DR, Campean V, et al. The lysyl oxidases LOX and LOXL2 are necessary and sufficient to repress E-cadherin in hypoxia: insights into cellular transformation processes mediated by HIF-1. *J Biol Chem* 2010;285:6658–69.
 35. Stamenkovic I, Yu Q. Shedding light on proteolytic cleavage of CD44: the responsible sheddase and functional significance of shedding. *J Invest Dermatol* 2009;129:1321–4.
 36. Kuphal S, Martyn AC, Pedley J, Crowther LM, Bonazzi VF, Parsons PG, et al. H-cadherin expression reduces invasion of malignant melanoma. *Pigment Cell Melanoma Res* 2009;22:296–306.
 37. Sarrío D, Palacios J, Hergueta-Redondo M, Gomez-Lopez G, Cano A, Moreno-Bueno G. Functional characterization of E- and P-cadherin in invasive breast cancer cells. *BMC Cancer* 2009;9:74.
 38. Tseng RC, Lee SH, Hsu HS, Chen BH, Tsai WC, Tzao C, et al. SLIT2 attenuation during lung cancer progression deregulates beta-catenin and E-cadherin and associates with poor prognosis. *Cancer Res* 2010;70:543–51.
 39. Halfon S, Abramov N, Grinblat B, Ginis IO. Markers distinguishing mesenchymal stem cells from fibroblasts are downregulated with passaging. *Stem Cells Dev* 2011;20:53–66.
 40. Peng L, Ran YL, Hu H, Yu L, Liu Q, Zhou Z, et al. Secreted LOXL2 is a novel therapeutic target that promotes gastric cancer metastasis via the Src/FAK pathway. *Carcinogenesis* 2009;30:1660–9.
 41. Moreb JS, Baker HV, Chang LJ, Amaya M, Lopez MC, Ostmark B, et al. ALDH isozymes downregulation affects cell growth, cell motility and gene expression in lung cancer cells. *Mol Cancer* 2008;7:87.
 42. Yang Y, Ahn YH, Gibbons DL, Zang Y, Lin W, Thilaganathan N, et al. The Notch ligand Jagged2 promotes lung adenocarcinoma metastasis through a miR-200-dependent pathway in mice. *J Clin Invest* 2011;121:1373–85.
 43. Anasagasti MJ, Alvarez A, Martin JJ, Mendoza L, Vidal-Vanaclocha F. Sinusoidal endothelium release of hydrogen peroxide enhances very late antigen-4-mediated melanoma cell adherence and tumor cytotoxicity during interleukin-1 promotion of hepatic melanoma metastasis in mice. *Hepatology* 1997;25:840–6.
 44. Cheng J, Zhou L, Xie QF, Xie HY, Wei XY, Gao F, et al. The impact of miR-34a on protein output in hepatocellular carcinoma HepG2 cells. *Proteomics* 2010;10:1557–72.
 45. Burk U, Schubert J, Wellner U, Schmalhofer O, Vincan E, Spaderna S, et al. A reciprocal repression between ZEB1 and members of the miR-200 family promotes EMT and invasion in cancer cells. *EMBO Rep* 2008;9:582–9.
 46. Gregory PA, Bert AG, Paterson EL, Barry SC, Tsykin A, Farshid G, et al. The miR-200 family and miR-205 regulate epithelial to mesenchymal transition by targeting ZEB1 and SIP1. *Nat Cell Biol* 2008;10:593–601.